

Hundred-gram Scale Fabrication of Few-layered Silicene by Continuous Vapor-Dealloying Strategy for High-Performance Lithium Storage

Xiaowei Wang,^a Jianmin Feng,^{b*} Feng Hou,^a Lei Dong,^b Conglai Long,^b Dejun Li,^b and Ji Liang^{a*}

- a. Key Laboratory of Advanced Ceramics and Machining Technology of Ministry of Education, School of Materials Science and Engineering, Tianjin University, Tianjin 300072, China.
- b. College of Physics and Materials Science, Tianjin Normal University, No 393 Bin Shui West Road, Xiqing District, Tianjin 300387, China.

Table of contents

1. Vapor-Dealloying Preparation of Silicene

2. The Application of Silicene for Lithium Storage

3. Cyclic Voltammetry (CV) and Galvanostatic Intermittent Titration Technique (GITT) analysis

4. Supporting Figures

1. Vapor-Dealloying Preparation of Silicene

Sample preparation. The fabrication of was conducted in a semi-continuous pyrolysis reactor consisting of a vertically oriented quartz tube and a horizontal quartz tube, heating by two separate tube furnaces, denoted as Furnace A and Furnace B (Figure S1). Polyvinyl chloride (PVC, K-value 62-60, aladdin) ((C₂H₃Cl)_n) was used as the etchant and the carbon source, which was fed into the Furnace A using spiral feeding way at a feed rate of 480 g/h. Furnace A was heated to 300 °C. PVC was pyrolysis into HCl gas, hydrocarbon gas, and residual carbon.

An argon flow was gone through Furnace A at a flow rate of 100 ml/min. The pyrolytic gas (HCl gas and hydrocarbon gas) flowed from Furnace A to Furnace B. In Furnace B, calcium silicide (CaSi₂, 95%, Gelest) was used as silicon source and was put in the constant temperature zone. Furnace B was heated to 600 °C. Under this condition, HCl gas will react with CaSi₂ to form CaCl₂ and nanolayered silicene. Partial hydrocarbon gas converted into pyrolysis carbon coating on silicene. The as-prepared product from Furnace B was washed by pure water to remove CaCl₂, and few-layered silicene was obtained. This vapor dealloying strategy can be further extended to other metal silicides, replaced CaSi₂ with MgSi₂ or AlSi₂, and nanoporous silicon will be obtained.

Materials Characterization. SEM observations and EDS analysis (SEM, TDCLS-8010, Hitachi Japan) was conducted as follows: the as-prepared product was dispersed in ethanol and dipped onto conductive tape as the analysis sample. In the same way, the as-prepared product ethanol solution was dropped copper grids coating with carbon film for TEM observation and EDX analysis (TEM, Talos F200X, FEI, US). The structure of the as-prepared products was analyzed by X-ray diffraction (XRD, D8 Advance, Bruker, German) and Raman spectroscopy (Horiba Jobin Yvon, LabRAM HR800, 17 mW, 514 nm, He-Ne laser), respectively. The surface chemistry of silicene

was analyzed by X-ray photoelectronic spectroscopy (XPS, Perkin-Elmer, PHI-1600, US).

2. The Application of Silicene for Lithium Storage

Silicene (20 mg) was put into 200 ml n-methyl-pyrrolidone (NMP), and an ultrasonic probe was applied to disperse it. After 1 hour's dispersion by an ultrasonic probe, 8.5 mg CNT was added, and the mixed solution was dispersed for another two hours. Then, the dispersed solution was pumped into films with a positive pressure filter device. Then, the film was pulled off and dried at 60 °C for 12 hours in a vacuum oven.

The counter electrode was a disk of lithium metal, and the separator is Celgard 2400. The electrolyte was 1 M LiPF₆ dissolved in a mixture of diethyl carbonate and ethylene carbonate (1:1 in volume) with 6% (volume ratio) Fluoroethylene carbonate additives. The assembly of the coin-type half-cells was carried out in a glove box whose contents of H₂O and O₂ were less than 0.1 ppm. Cyclic Voltammetry (CV) analysis was carried out with a Princeton electrochemical workstation. Galvanostatic charge/discharge and Galvanostatic Intermittent Titration Technique (GITT) testing were conducted in the voltage range of 0.01–3.0 V (vs. Li/Li⁺) using a LAND multichannel battery test system.

3. Cyclic Voltammetry (CV) and Galvanostatic Intermittent Titration

Technique (GITT) analysis

The electrochemical behavior of the few-layered silicene towards Li storage has been further investigated using cyclic voltammetry (CV) and galvanostatic intermittent titration technique (GITT). The CV curves under various scanning rates from 0.1 to 0.8 mV s⁻¹ display similar but higher cathodic/anodic peaks intensity during lithiation/delithiation processes with the increase of scanning rates (**Fig. S12a**). It is known that the lithium intercalation in the electrode during the

charge process consists of two processes: the diffusion-controlled faradic process and the surface-reaction-controlled capacitive process. The specific contribution of each part can be quantified according to the equation:

$$i = k_1v + k_2v^{1/2}$$

or

$$i/v^{1/2} = k_1v^{1/2} + k_2$$

where i is the response current at different potentials, v is the scanning rate, and k_1 , k_2 are constants. At a given potential, the terms k_1v and $k_2v^{1/2}$ represent the current response due to the capacitive process and diffusion-controlled faradaic process, respectively. The k_1 and k_2 can be calculated by plotting $i/v^{1/2}$ vs. $v^{1/2}$, thus the fraction of the charge from the capacitive process and diffusion-controlled process could be determined.

As shown in **Fig. S12b**, the capacitive process contribution of silicene is 67.59% and the diffusion process contributes 32.41% of the total capacity, respectively. The diffusion-controlled charge storage on silicene mainly occurs at the low and middle potential region that is lower than 1 V. Contribution ratios between the two processes under different scan rates were also quantified. **Fig. S12c** shows that the capacitive current ratio increased gradually with the increase of scanning rates, from 43.30% at 0.1 mV s⁻¹ to 67.59% at 0.8 mV s⁻¹ (**Fig. S13**). The high ratio capacitive lithium storage contribution of silicene indicates the adsorption and migration lithium storage mechanism.

Then, GITT was conducted, and the diffusion coefficient, voltage, and capacity were plotted in

Fig. S12d. The diffusion coefficient in the charging process increases with the potential. It reaches the highest value ($8.1 \times 10^{-12} \text{ cm}^2 \text{ S}^{-1}$) at around 0.6 V, consisting of the oxidation peaks in the CV loop and indicating the reaction at the platform possesses more dynamic advantages. The diffusion coefficient in the discharge process is consistent with the trend in the reduction part in the CV loop, demonstrating the peak value at around 0.2 V.

CV and GITT analysis showed that there is a high capacitive contribution in the lithium storage in silicene. It could be speculated that the two-dimensional structure of silicene is conducive to the rapid adsorption and migration of lithium-ions.

4. Supporting Figures

Figure S1. Schematic diagram of synthesis equipment of silicene and photograph of silicene (inset).

Figure S2. SEM image of silicene/ CaCl_2

Figure S3. SEM image of silicene/carbon product using cable sheath as hydrogen chloride sources and photographs of raw materials and annealing products (inset).

Figure S4. **a)** Schematic diagram of synthesis of porous Si, **b)** SEM images of porous Si from Mg_2Si (inset), **c)** SEM image of porous Si from Al/Si alloy (inset).

Figure S5. **a, b)** XRD patterns of the produces derived from Mg_2Si **a** and Si/Al alloy **b** precursors, **c)** SEM image of the porous silicon derived from Mg_2Si , **d-f)** the corresponding TEM image and elemental mapping of Si and C, **g)** SEM image of porous silicon derived from Al/Si alloy, **h-j)** the corresponding TEM image and elemental mapping of Si and C.

Figure S6. **a)** High-resolution STEM image of the amorphous area and corresponding Fourier transform diagram, **b)** XPS survey spectra of the silicene.

Figure S7. **a)** SEM image of the silicene particle in silicene@CNT film, **b)** high-resolution SEM image of silicene in CNT net.

Figure S8. **a)** Photograph of the folding silicene@CNT-FS film, **b)** releasing film.

Figure S9. **a)** CNT free-standing film from chemical vapor deposition and rate performance (inset), **b)** charge/discharge curves of 1st, 10th, 20th, 30th and 40th cycle.

Figure S10. **a)** the initial charge-discharge curves for silicene@CNT-FS, **b)** relevant charge-discharge curves under different current densities in **Figure 4f**.

Figure S11. **a)** TEM image of silicene@CNT 1 after 500 cycle, **b-d)** EDS mapping of C, Si, and O element in the selected area.

Figure S12. **a)** CV curves of silicene upon lithiation at various scanning rates, **b)** separation of the capacitive and diffusion currents in silicene at a scan rate of 0.8 mV s^{-1} , **c)** contribution ratio of the capacitive and diffusion-controlled charge versus scan rate, **d)** GITT based calculation diffusivity under different potential and corresponding charge-discharge curves.

Figure S13. Contribution ratio of the capacitive and diffusion-controlled charge versus scan rate of **a)** 0.5 mV s^{-1} , **b)** 0.3 mV s^{-1} , **c)** 0.2 mV s^{-1} , **d)** 0.1 mV s^{-1} .

Figure S1.

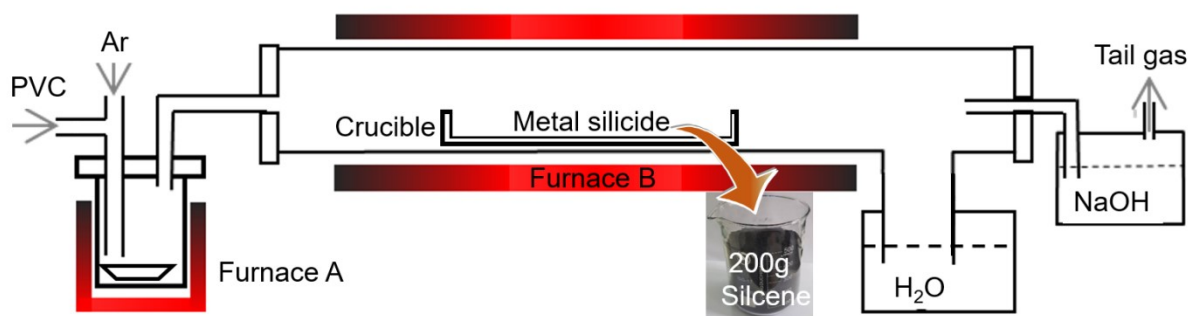


Figure S2.

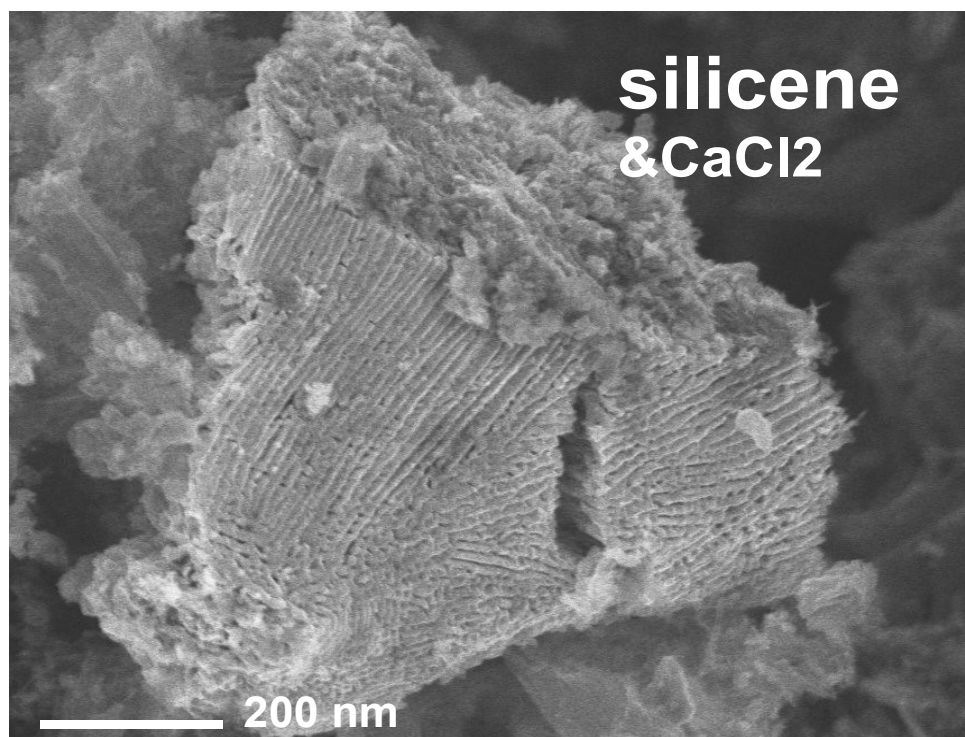


Figure S3.

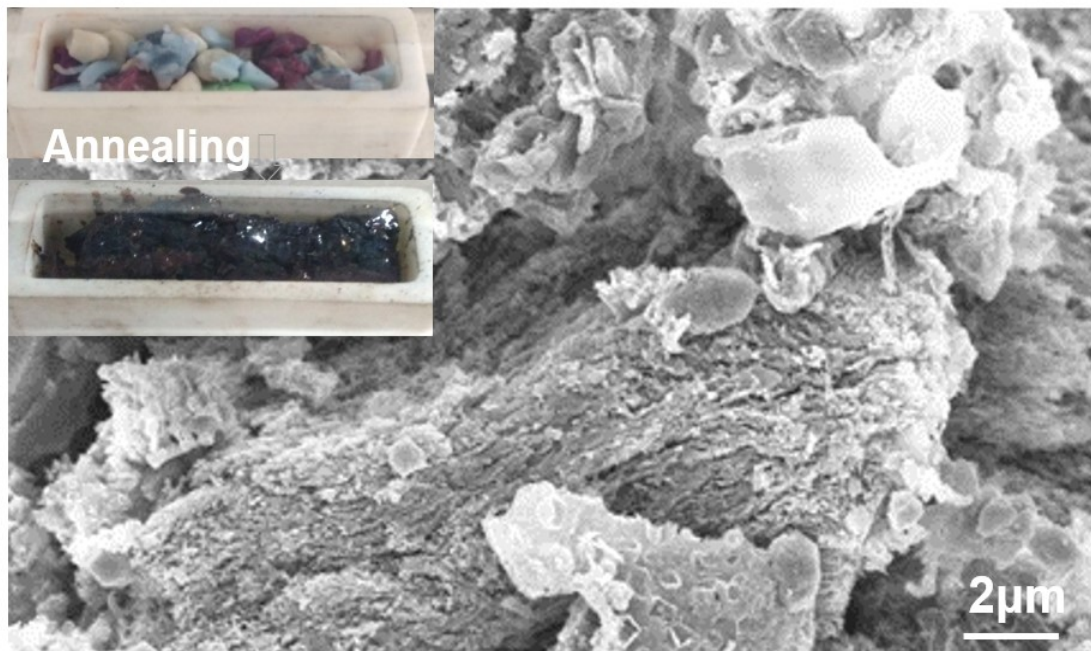


Figure S4.

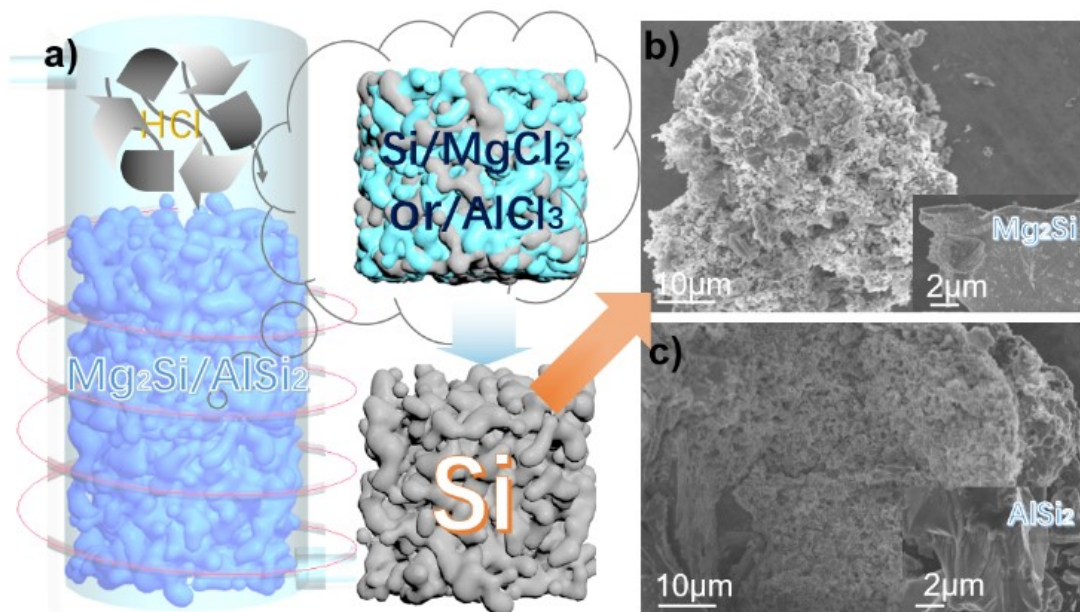


Figure S5.

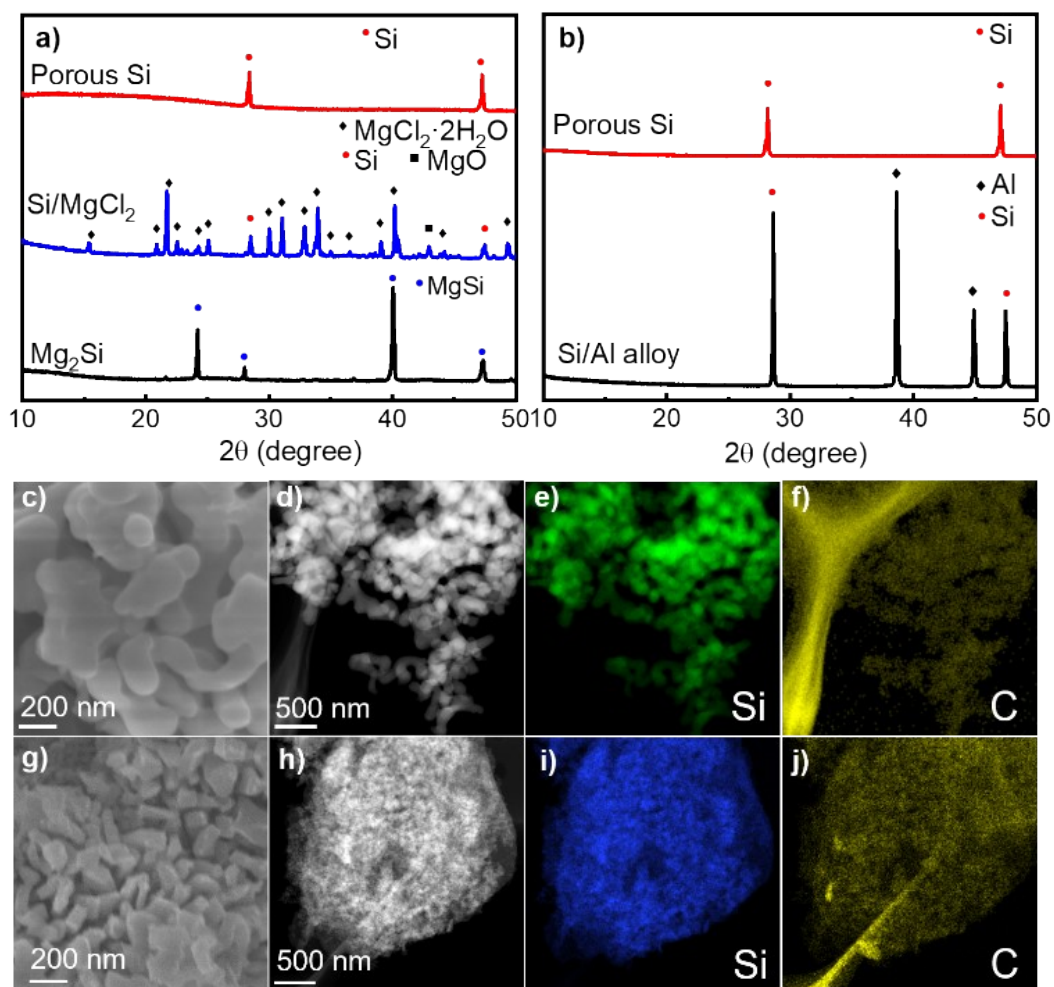


Figure S6.

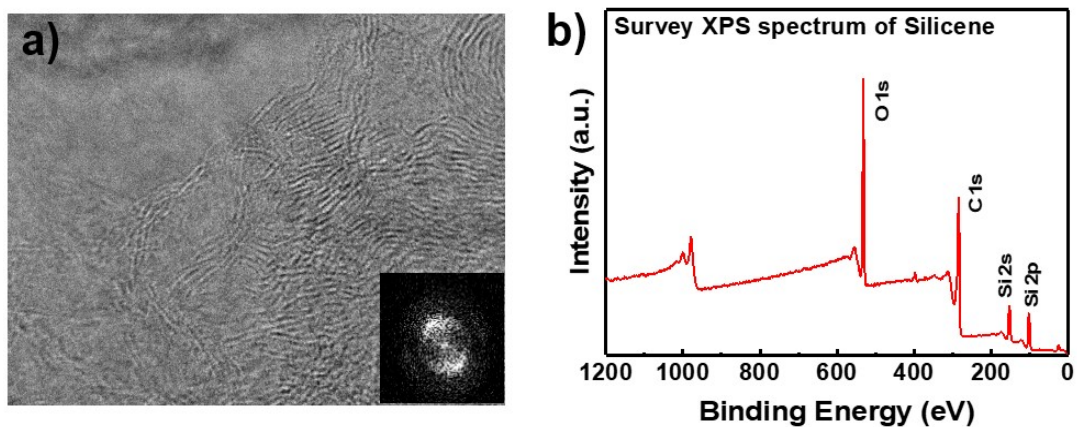


Figure S7.

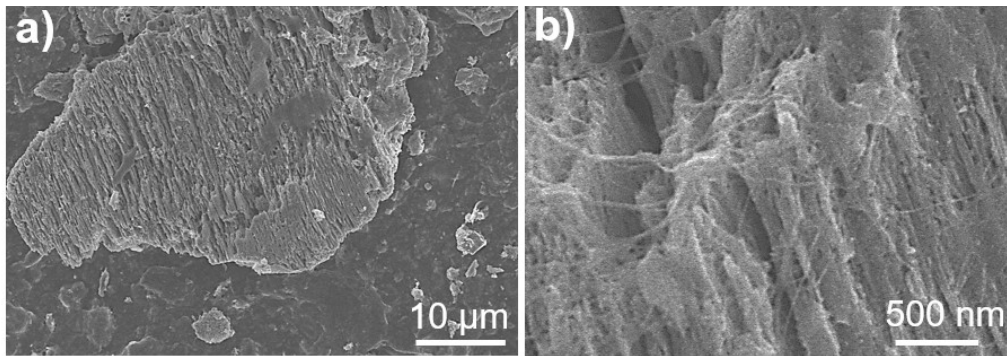


Figure S8.

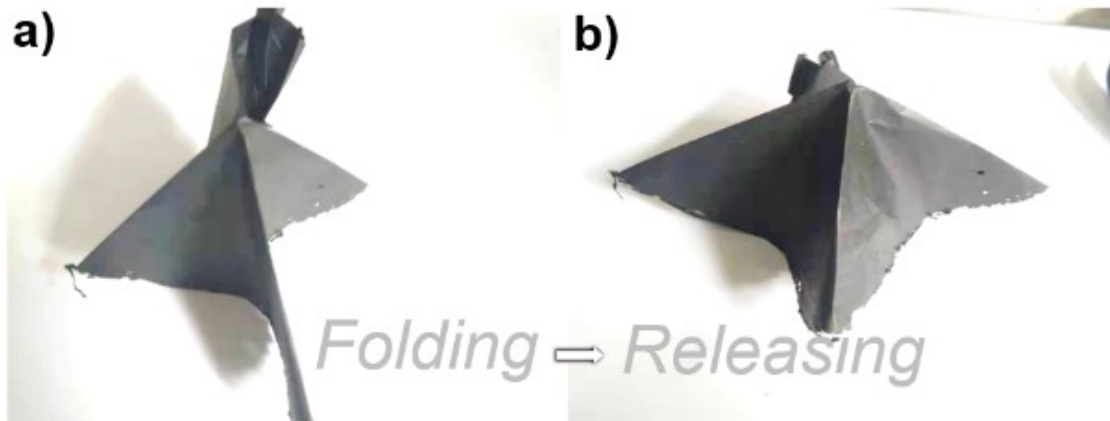


Figure S9.

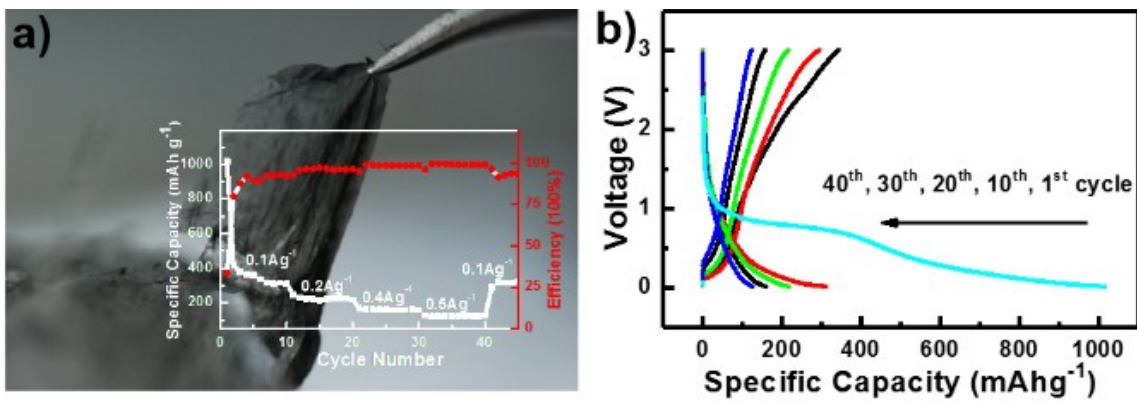


Figure S10.

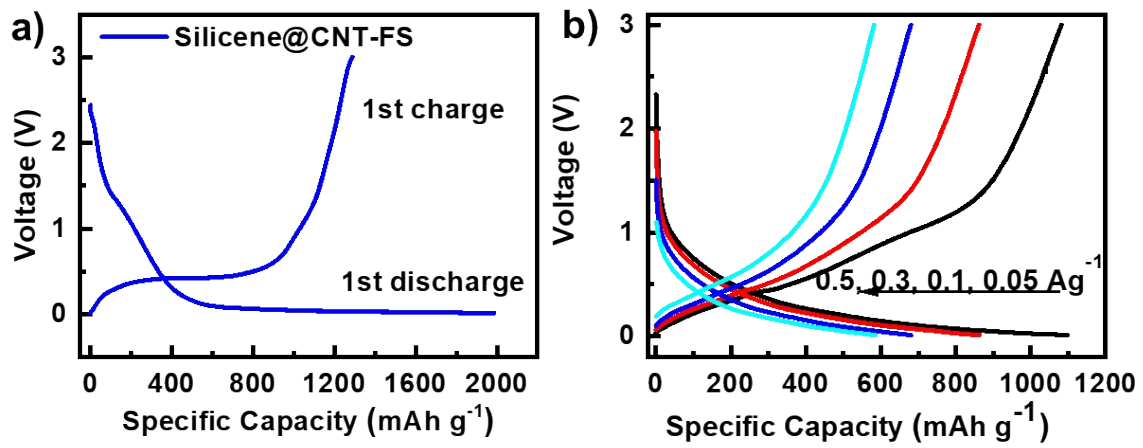


Figure S11.

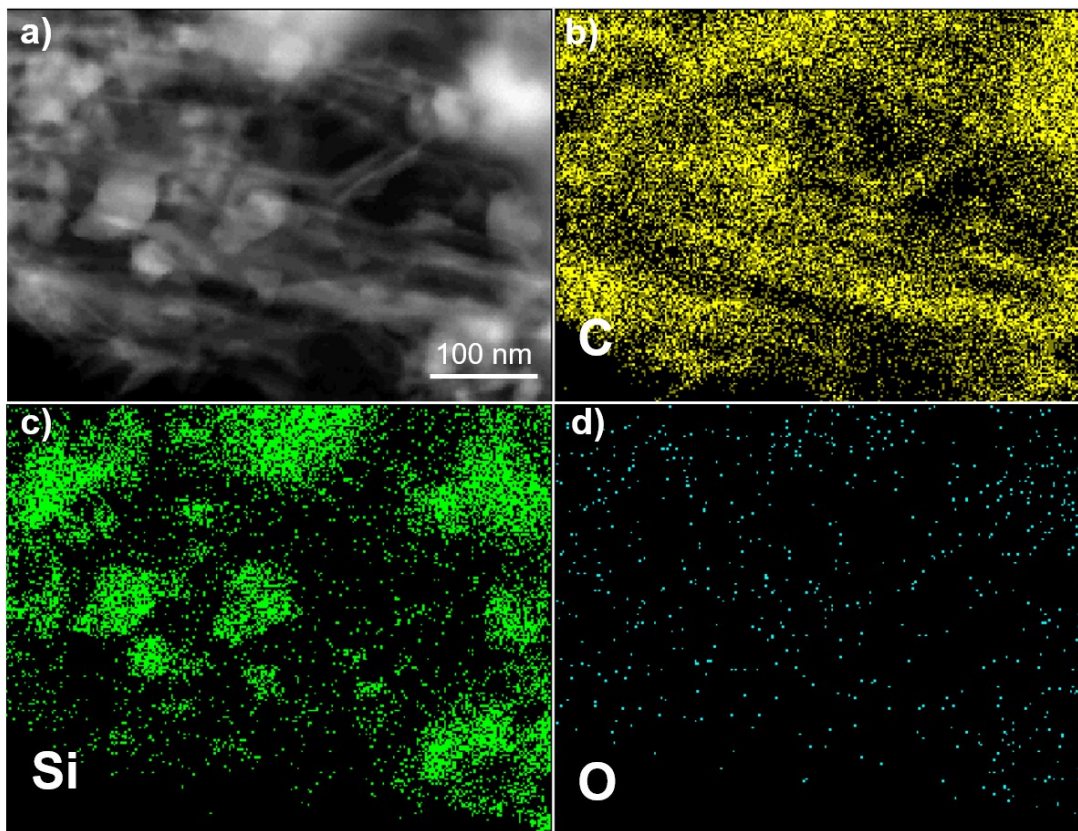


Figure S12.

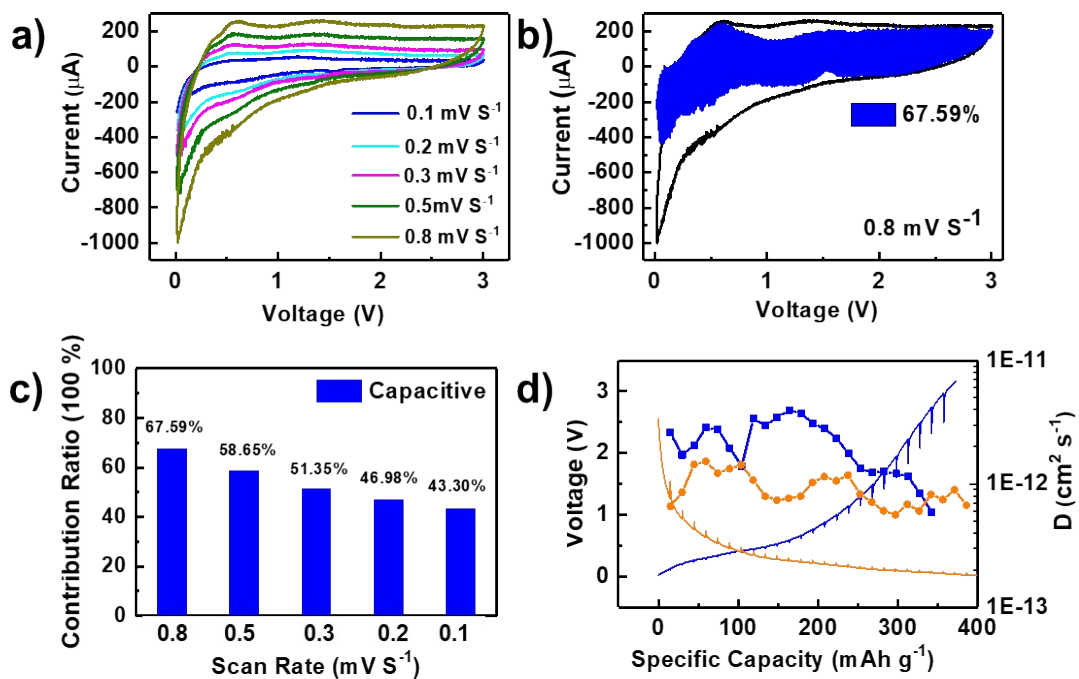


Figure S13.

